

Published in final edited form as:

*Langmuir*. 2013 August 27; 29(34): 10868–10873. doi:10.1021/la402425n.

## Fabrication of DNA Microarrays on Polydopamine-Modified Gold Thin Films for SPR Imaging Measurements

Jennifer B. Wood, Megan W. Szyndler, Aaron R. Halpern, Kyunghee Cho, and Robert M. Corn

Department of Chemistry, University of California-Irvine, Irvine, CA 92697, USA

### Abstract

Polydopamine (PDA) films were fabricated on thin film gold substrates in a single-step polymerization-deposition process from dopamine solutions and then employed in the construction of robust DNA microarrays for the ultra-sensitive detection of biomolecules with nanoparticle-enhanced surface plasmon resonance (SPR) imaging. PDA multilayers with thicknesses varying from 1 to 5 nm were characterized with a combination of scanning angle SPR and AFM experiments, and  $1.3 \pm 0.2$  nm PDA multilayers were chosen as an optimal thickness for the SPR imaging measurements. DNA microarrays were then fabricated by the reaction of amine-functionalized single-stranded DNA (ssDNA) oligonucleotides with PDA-modified gold thin film microarray elements, and were subsequently employed in SPR imaging measurements of DNA hybridization adsorption and protein-DNA binding. Concurrent control experiments with noncomplementary ssDNA sequences demonstrated that the adhesive PDA multilayer was also able to provide good resistance to the nonspecific binding of biomolecules. Finally, a series of SPR imaging measurements of the hybridization adsorption of DNA-modified gold nanoparticles onto mixed sequence DNA microarrays were used to confirm that the use of PDA multilayer films is a simple, rapid and versatile method for fabricating DNA microarrays for ultrasensitive nanoparticle-enhanced SPR imaging biosensing.

### Introduction

Polydopamine (PDA), a synthetic polymer inspired by the adhesive proteins produced by mussels in marine environments, is a uniquely reactive adhesive thin film coating that has been incorporated into a variety of materials applications.<sup>1,2</sup> The ability of mussels to adhere to both inorganic and organic surfaces relies upon adhesive proteins that are rich in 2,4-dihydroxy-L-phenylalanine (DOPA) residues.<sup>3</sup> Messersmith, *et al.* demonstrated that the related molecule dopamine could serve as a suitable monomer for the formation of adhesive polymeric coupling layers on numerous substrates.<sup>2</sup> The selfpolymerization of dopamine, which contains both a catechol and an amine, is proposed to occur in the presence of oxygen in slightly basic aqueous conditions via the covalent sequential linking of monomers followed by further aggregation via  $\pi$ -stacking interactions.<sup>4,5</sup> The formation of a stable, water-resistant PDA thin film is a rapid one-step process that requires minimal reagents and mild reaction conditions. Examples of the uses of PDA thin films include: the coating of superparamagnetic nanoparticles<sup>6</sup> and the incorporation of nanoparticles into thin PDA films for immunoassays,<sup>7</sup> the encapsulation of living cells,<sup>8</sup> and the imprinting of proteins into PDA nanowires for biosensing applications.<sup>9</sup>

In this paper, PDA multilayer films are formed in a single-step polymerization-deposition process from dopamine solutions and then used to covalently attach single-stranded DNA (ssDNA) oligonucleotides onto the DNA microarrays. Under slightly basic conditions, the equilibrium between catechols and *o*-quinones in PDA shifts toward the latter.<sup>1</sup> This enables the conjugation of biomolecules that contain amine functional groups onto PDA-coated substrates via Michael addition or Schiff base reactions.<sup>10,11</sup> PDA amine attachment chemistry has been shown to be better at withstanding hydrolysis as compared to the standard EDC/NHS coupling<sup>12</sup> of amine-terminated biomolecules to carboxylic acid-modified surfaces.<sup>13</sup> This PDA chemistry is used to attach amine-modified ssDNA oligonucleotides (30 mers) onto gold thin film microarray elements.

Surface plasmon resonance (SPR) imaging measurements of the DNA microarrays are employed to monitor the effectiveness of the PDA surface attachment chemistry. DNA microarrays have been applied extensively both in biomolecular research and clinical application settings,<sup>14–18</sup> and are used to detect and identify (i) specific DNA target sequences in solution via hybridization adsorption, and (ii) DNA-binding proteins via specific bioaffinity adsorption onto the microarray. The optical technique of SPR imaging is a highly effective method for detecting bioaffinity adsorption onto the DNA microarray via changes in the local refractive index.<sup>19–1</sup> SPR imaging measurements are also used to show that the adhesive PDA layer provides good resistance to nonspecific binding of non-complementary target biomolecules onto the DNA microarray elements.

An additional application of DNA microarrays created with the PDA surface attachment chemistry demonstrated in this paper is the detection of DNA and RNA at extremely low (femtomolar) concentrations with nanoparticle-enhanced SPR imaging measurements.<sup>22,23</sup> In these measurements, the hybridization adsorption of DNA or RNA-modified gold or silica nanoparticles onto DNA microarrays must be quantitated at extremely low (< 0.5%) surface coverages.<sup>23</sup> DNA microarrays that contain diluted ssDNA target sequences are fabricated with the one-step PDA surface attachment chemistry, and then used in a series of SPR imaging measurements to quantitate the specific adsorption of DNA-functionalized nanoparticles.

## Experimental Section

### Materials

Polydopamine (PDA) coating was performed using dopamine hydrochloride (Sigma-Aldrich) dissolved in 10 mM Tris buffer (Trizma hydrochloride; Sigma-Aldrich) at pH 8.5. Microarray chips (16 spots, 1.0 mm diameter) for SPR imaging experiments were prepared by thermally evaporating (Denton DV 502-A evaporator) 45 nm of gold, with 1 nm of chromium underneath as an adhesion layer, onto SF10 glass slides (18 × 18 mm; Schott Glass).

### Nucleic Acids

Modified ssDNA oligonucleotides (Integrated DNA Technologies) were diluted in either 1X phosphate buffer (11.9 mM phosphates, 137 mM sodium chloride, 2.7 mM potassium chloride, pH 7.4; Fisher) for DNA hybridization and AuNP modification, or Tris buffer for ssDNA fabrication onto the PDA layer. Sequences of the ssDNA strands are listed in Table I. Single-stranded DNA binding protein (SSB; Epicenter Technologies) was used as received. All cleansing steps consisted of rinsing under absolute ethanol and/or Millipore filtered water, followed by drying under nitrogen. All experiments were performed at room temperature.

## Solutions

For DNA attachment: ssDNA (250  $\mu\text{M}$  A, B, C, D in Tris buffer). For DNA SPR imaging hybridization: ssDNA (1  $\mu\text{M}$  A<sub>C</sub>, D<sub>U</sub> in PBS buffer). For SSB binding: SSB (10 nM in PBS buffer).

## Gold Nanoparticles

Synthesis of ~13 nm gold nanoparticles by citrate reduction followed the Turkevich Method.<sup>24</sup> Briefly, H<sub>2</sub>AuCl<sub>4</sub> (0.0223 g, 0.0656 mmol) was dissolved in 100 mL water. Sodium citrate dihydrate (0.0533 g, 0.1812 mmol, in 5 mL water) was then added to the boiling solution. After a color change (from blue to red) was observed, the reaction solution continued to boil for ten more minutes.

## DNA-Modification of the Gold Nanoparticles

AuNP solution (1 mL) was filtered (0.22  $\mu\text{m}$ ) prior to the addition of 1 mM thiol-terminated ssDNA (5  $\mu\text{L}$ , in PBS buffer). After the mixture was kept at 37 °C for 24 hours, 500  $\mu\text{L}$  of PBS buffer was added to the solution. The solution was kept at 37 °C for another 24 hours to age the particles. Two centrifugation cycles (15800 rcf, 15 minutes) were applied to remove the excess ssDNA in the solution, followed by removal of supernatant and resuspension in PBS buffer. The nanoparticle concentrations were adjusted to approximately 3 nM. Measurements of AuNPs concentrations were done by UV-vis spectroscopy ( $\lambda_{\text{max}} = 520$  nm,  $2.7 \times 10^8 \text{ M}^{-1} \text{ cm}^{-1}$  as extinction coefficient).<sup>25</sup>

## Scanning Angle SPR Apparatus

The *ex situ* scanning angle SPR measurements were performed at 632.8 nm and a BK7 prism/substrate using a homebuilt apparatus that has been described previously.<sup>26</sup>

PDA solution (10.5 mM) flowed through a peristaltic pump over an Au surface (plain Au served as the unmodified reference). The PDA film was grown in 5-minute increments. Each growth step was followed by ten minute rinsing with water and drying under nitrogen. Data analysis provided the reflectivity minima and the calculated change in angle for each growth interval.

## Fabrication of ssDNA onto PDA Layer

Gold spots on the microarray chip were covered with 10.5 mM PDA solution for ten minutes. Subsequently, each gold spot was exposed to 0.5  $\mu\text{L}$  of 250  $\mu\text{M}$  amine-terminated ssDNA for 12 hrs.

## SPR Imaging Apparatus

Real-time measurements were conducted using an SPR imager (GWC Technologies) as described previously.<sup>27</sup>

## AFM Apparatus

Atomic force microscopy (AFM) measurements were obtained using an Asylum research, MFP-3D AFM with Olympus, AC160TS tips.

## Surface PDA Multilayer Formation

For the *in situ* SPR imaging measurements, millimolar dopamine solutions in a pH 8.5 Tris buffer were pumped through one channel of a dual 100  $\mu\text{L}$  flow cell over 8 of 16 elements in an SPR imaging microarray chip (each gold thin film microarray element was 45 nm in thickness and 1mm in diameter) at a flow rate of 0.3 mL/min. Simultaneously, the other 8

elements were exposed to dopamine-free Tris buffer via a second microfluidic channel, in order to serve as the control elements. Continuous PDA film growth was observed for dopamine concentrations ranging from 1.3 to 21 mM; 10.5 mM PDA was chosen as optimal, as it was the standard concentration used elsewhere.<sup>13</sup>

## Results and Discussion

### A. PDA Film Deposition: *In Situ* SPR Imaging Measurements

The polymerization-deposition of PDA multilayers onto gold thin films was monitored with real-time *in situ* SPR imaging measurements. This polymerization reaction occurred spontaneously in a 10.5 mM dopamine solution buffered to a pH 8.5. Figure 1 shows the real-time SPR imaging differential reflectivity data. In this experiment, PDA film growth was observed after exposing a gold microarray to alternating cycles of 5 minutes of dopamine solution and then 5 minutes of Tris buffer. The real-time changes in reflectivity (%R) were monitored and are shown in Figure 1 as the red curve; also shown in the figure is the real time %R from control elements that were only exposed to Tris buffer (blue curve). The polymerization of dopamine to form PDA both on the array surface and in solution produced a rapid increase in %R. When the dopamine solution was replaced by Tris buffer; the %R immediately dropped and remained constant. We attribute this initial drop in %R to the replacement of a dopamine solution that now contained PDA, and the steady-state increase in %R to the deposition of a PDA film that was irreversibly and directly attached to the gold surface. Further evidence of a solution polymerization reaction was that the dopamine solution eventually turned a light brown.<sup>2,28</sup> The dopamine/Tris buffer exposure cycle was repeated six times, and a total steady-state increase in %R of 40% was observed after 30 min of exposure time to dopamine solution ( $\text{Time}_{\text{exp}}$  in Figure 1). The inset in Figure 1 shows the linear dependence of the steady-state increase in %R with  $\text{Time}_{\text{exp}}$ . These SPR imaging measurements clearly indicate that the PDA film thickness on the gold surface could be controlled by deposition time.

### B. PDA Film Characterization: *Ex Situ* SPR and AFM Measurements

To further characterize the PDA film deposition process, a combination of *ex situ* 633 nm SPR scanning angle shift measurements and atomic force microscopy (AFM) measurements were performed. The *ex situ* scanning angle SPR curves at 633 nm of PDA films were obtained using reaction times of 10, 20 and 30 minutes are plotted in Figure 2 (red, green and blue curves, respectively). Also shown in the figure is the SPR curve for a bare gold surface (gray line). A linear shift in the SPR angle was observed as a function of reaction time (see the inset in the figure). The SPR curves from the PDA films also show a slight increase in the reflectivity at the SPR angle that is typical for thin films with a complex refractive index; this reflectivity increase was almost negligible at 833 nm, the wavelength of the SPR imaging measurements. Along with the *in situ* SPR imaging measurements, the linear shift in the SPR angle verifies that we can control the PDA film thickness by varying the deposition time. Additionally, the thickness of the ten minute PDA film was measured with AFM measurements (see the Supplementary Information) and was determined to be  $1.3 \pm 0.2$  nm. We use a ten minute PDA film deposition time to fabricate all of the ssDNA microarrays in the subsequent SPR imaging measurements.

### C. SPR Imaging Measurements of DNA Microarrays Fabricated by PDA Attachment Chemistry

**1. Surface attachment chemistry and microarray fabrication**—In order to create ssDNA SPR imaging microarrays, a  $1.3 \pm 0.2$  nm PDA film was simultaneously deposited onto all gold microarray elements, and then an amine-terminated ssDNA was reacted with the PDA on each gold spot (the sequences of the ssDNA are listed in Table I). PDA

multilayers have been used by several researchers to attach amine-labeled biomolecules onto surfaces.<sup>1</sup> Sixteen element, 1 mm diameter gold spot microarrays were used in the SPR imaging measurements.<sup>27</sup> Each PDA-modified gold microarray element was exposed to 0.5  $\mu\text{L}$  of 250  $\mu\text{M}$  amine-terminated ssDNA solution for twelve hours and then the microarray was rinsed with water and dried under nitrogen.

**2. DNA hybridization adsorption experiments**—To determine the quality of the ssDNA microarrays fabricated with PDA, the sequence-specific adsorption of complementary ssDNA (denoted as "hybridization adsorption") onto the ssDNA microarrays was monitored with SPR imaging. A 16-element SPR imaging chip that contained two sequences, A and B, was fabricated as shown in Figure 3. The microarray was then exposed to a 1.0  $\mu\text{M}$  solution of ssDNA complementary to sequence A (denoted as  $A_C$ ) for 8 minutes; real-time SPR imaging reflectivity curves were recorded and are plotted in Figure 3 (solid red curve, A elements; dotted blue curve, B elements). For the A elements, there was a significant increase in %R of  $2.5 \pm 0.3\%$  due to the hybridization adsorption of  $A_C$ . This %R of 2.5% due to hybridization adsorption is similar to that obtained in previous SPR imaging measurements on DNA microarrays.<sup>26</sup> Using those previous measurements, we can estimate that the PDA-modified surfaces created an active ssDNA monolayer with a surface density of  $2 \pm 1 \times 10^{12}$  molecules/ $\text{cm}^2$ .<sup>26</sup> This result suggests that the surface coverage of reactive sites on the PDA film is similar to that observed on pGlu-modified gold substrates.<sup>26</sup> Most hybridization adsorption measurements utilize ssDNA monolayers at this surface coverage or less, in order to optimize hybridization efficiency. This value is approximately 5 to 10 times less than the maximum ssDNA surface density of  $10^{13}$  molecules/ $\text{cm}^2$  that has been observed with DNA-alkanethiol monolayers.<sup>29</sup>

As seen in Figure 3, no increase in %R was observed for the B microarray elements ( $0.0 \pm 0.1\%$ ). The lack of any adsorption of  $A_C$  onto the non-complementary ssDNA monolayer indicates that there was nearly no non-specific DNA adsorption. This result agrees with previous reports showing the ability of PDA-modified surfaces to resist non-specific adsorption.<sup>2</sup>

**3. SSB adsorption experiments**—In a second set of experiments, the specific bioaffinity adsorption of single-stranded DNA binding protein (SSB) onto the DNA microarray was monitored with SPR imaging. A two-component ssDNA microarray was fabricated using the PDA attachment chemistry consisting of the sequences C ( $A_{30}$ ) and D ( $T_{30}$ ). The microarray was first exposed to a 1  $\mu\text{M}$  solution of sequence  $D_U$ , which is complementary to C, to form a dsDNA monolayer on half of the array elements. The microarray was then exposed to a 10 nM SSB solution; the SPR imaging reflectivity curves were recorded and are plotted in Figure 4. A large increase in %R ( $10.5 \pm 0.3\%$ ) was observed for the D elements; this is attributed to the adsorption of SSB onto the ssDNA monolayer. The %R value is similar to the value observed in previous SPR imaging microarray measurements, and is reasonable considering the significant size of SSB (~75 kDa).<sup>26</sup>

As seen in Figure 4, only a minimal amount of adsorption was observed on the dsDNA microarray elements after 50 min ( $0.4 \pm 0.04\%$  %R). The fact that the dsDNA layer was able to completely block the adsorption of SSB suggests that there is almost 100% surface hybridization efficiency of complementary ssDNA onto these microarray elements. These results conclusively demonstrate that DNA microarrays created by this PDA attachment chemistry should be applicable to the study of DNA-protein interactions.

## D. Nanoparticle-Enhanced SPR Imaging Measurements

In a final set of experiments, DNA microarrays fabricated by the PDA attachment chemistry were used to quantitate the hybridization adsorption of DNA-functionalized gold nanoparticles (AuNPs) for nanoparticle-enhanced SPR imaging measurements. Nanoparticle-enhanced SPR imaging has been used in a number of ultrasensitive SPR imaging detection schemes.<sup>22,23,30</sup> For these measurements, it is typically necessary to detect minute surface coverages of complementary DNA by the hybridization adsorption of DNA-functionalized AuNPs. To test the capability of the PDA attachment chemistry, 16-element DNA microarrays were fabricated in which each microarray element contained a mixed ssDNA monolayer with a distinct ratio of two sequences (D and B). Figure 5 shows an example of a DNA microarray in which the percentage of sequence D in the monolayer was varied from 0, 1, 5, 10, 15, 20, 30, 100%. The SPR imaging difference image in the figure was obtained after exposure to a  $3.2 \pm 0.5$  nM solution of AuNPs functionalized with ssDNA complementary to D (sequence C<sub>T</sub>).

Figure 6 plots the compiled results of multiple SPR imaging measurements of the hybridization adsorption of DNA-functionalized AuNPs onto mixed monolayer microarrays with %D ranging from 0.1 to 30%. A maximum reflectivity of  $50 \pm 1$  %R is observed for %D of 30% (%R is saturated for the surfaces with %D over 30%), indicating the hybridization of a full monolayer of AuNPs. Below a %D of 30%, the %R dropped monotonically, at concentrations below a %D of 1%, %R was linear with %D. The lowest %D for which that could be measured was 0.1% D for which the %R was  $1.08 \pm 0.3\%$ . This robust DNA microarray with PDA chemistry detected the ssDNA modified AuNPs down to 0.1% surface coverage of D. Additional elements, which contained no sequence D, were used as controls for non-specific adsorption, and gave a %R of  $0.17 \pm 0.06\%$ .

These mixed monolayer measurements can be used to estimate the sensitivity of nanoparticle-enhanced SPR imaging measurements with these DNA microarrays. As described in our previous work, the relative surface coverage  $\theta = \theta / \theta_{\max}$  of hybridized DNA is related to the solution concentration via the Langmuir adsorption constant  $K_{\text{ads}}$ , which is approximately  $10^8 \text{ M}^{-1}$ .<sup>22,26,31</sup> At low concentrations, this relationship is linear, and the minimum detectable solution concentration ( $C_{\min}$ ) is related to the minimum detectable surface coverage  $\theta_{\min}$  by Equation 1:

$$\theta_{\min} = K_{\text{ads}} C_{\min} \text{ for } K_{\text{ads}} C_{\min} \ll 1 \quad (1)$$

The minimum %D obtained in the mixed monolayer measurements was 0.1%, which corresponds to a  $\theta_{\min}$  of  $10^{-3}$ . Using Eqn 1, we can estimate that the minimum concentration one should be able to see in nanoparticle-enhanced SPR imaging measurements is  $\theta_{\min}/K_{\text{ads}} = 10 \text{ pM}$ . This number is comparable to that observed in previous nanoparticle-enhanced SPR imaging measurements.<sup>22</sup>

## IV. Conclusions

The paper describes and demonstrates the use of PDA thin films on gold surfaces as a key component in the construction of robust ssDNA microarrays for SPR imaging biosensing measurements. The fabricated ssDNA microarrays were stable and exhibited excellent bioavailability to both nucleic acids and proteins in solution. From the SPR imaging measurements of DNA hybridization adsorption and SSB binding, we estimate that the PDA chemistry creates a highly bioactive ssDNA film with a surface coverage of  $2 \times 10^{12}$  molecules/cm<sup>-2</sup>. Additionally, mixed ssDNA monolayers were used to detect the hybridization adsorption of AuNPs onto elements that contained a percentage of complementary ssDNA as low as 0.1%; these measurements demonstrate the viability of the

ssDNA microarrays for ultrasensitive nucleic acid biosensing with nanoparticle-enhanced SPR imaging. In all of the measurements utilizing PDA thin films, negligible nonspecific adsorption was observed.

These SPR imaging measurements suggest that the use of ssDNA microarrays created by the attachment of amine-terminated ssDNA onto PDA films can be extended to various biosensing methodologies, such as miRNA detection and the use of DNAzyme and aptamers for protein detection.<sup>23,32</sup> Future studies will explore the use of PDA films at higher temperatures for use in conjunction with surface enzymatic amplification strategies,<sup>30</sup> and we also plan to gain a finer spatial control over the PDA deposition process through the use of electropolymerization.<sup>33</sup>

## Supplementary Material

Refer to Web version on PubMed Central for supplementary material.

## Acknowledgments

This work was supported by the NIH through grant R01-GM059622.

## References

1. Lyngø ME, van der Westen R, Postma A, Stadler B. Polydopamine—a Nature-Inspired Polymer Coating for Biomedical Science. *Nanoscale*. 2011; 3:4916. [PubMed: 22024699]
2. Lee H, Dellatore SM, Miller WM, Messersmith PB. Mussel-Inspired Surface Chemistry for Multifunctional Coatings. *Science*. 2007; 318:426. [PubMed: 17947576]
3. Waite JH, Qin X. Polyphosphoprotein from the Adhesive Pads of *Mytilus Edulis*. *Biochemistry*. 2001; 40:2887. [PubMed: 11258900]
4. d'Ischia M, Napolitano A, Pezzella A, Meredith P, Sarna T. Chemical and Structural Diversity in Eumelanins: Unexplored Bio-Optoelectronic Materials. *Angew. Chem. Int. Ed.* 2009; 48:3914.
5. Dreyer DR, Miller DJ, Freeman BD, Paul DR, Bielawski CW. Elucidating the Structure of Poly(Dopamine). *Langmuir*. 2012; 28:6428. [PubMed: 22475082]
6. Zhou W, Lu C, Guo X, Chen F, Yang H, Wang X. Mussel-Inspired Molecularly Imprinted Polymer Coating Superparamagnetic Nanoparticles for Protein Recognition. *J. Mater. Chem.* 2010; 20:880.
7. Fu Y, Li P, Wang T, Bu L, Xie Q, Xu X, Lei L, Zou C, Chen J, Yao S. Novel Polymeric Bionanocomposites with Catalytic Pt Nanoparticles Label Immobilized for High Performance Amperometric Immunoassay. *Biosens. Bioelectron.* 2010; 25:1699. [PubMed: 20056402]
8. Yang SH, Kang SM, Lee K, Chung TD, Lee H, Choi IS. Mussel-Inspired Encapsulation and Functionalization of Individual Yeast Cells. *J. Am. Chem. Soc.* 2011; 133:2795. [PubMed: 21265522]
9. Ouyang R, Lei J, Ju H. Surface Molecularly Imprinted Nanowire for Protein Specific Recognition. *Chem. Commun.* 2008; 0:5761.
10. Burzio LA, Waite JH. Cross-Linking in Adhesive Quinoproteins: Studies with Model Decapeptides. *Biochemistry*. 2000; 39:11147. [PubMed: 10998254]
11. LaVoie MJ, Ostaszewski BL, Weihofen A, Schlossmacher MG, Selkoe DJ. Dopamine Covalently Modifies and Functionally Inactivates Parkin. *Nat. Med.* 2005; 11:1214. [PubMed: 16227987]
12. Sehgal D, Vijay IK. A Method for the High Efficiency of Water-Soluble Carbodiimide-Mediated Amidation. *Anal. Biochem.* 1994; 218:87. [PubMed: 8053572]
13. Lee H, Rho J, Messersmith PB. Facile Conjugation of Biomolecules onto Surfaces Via Mussel Adhesive Protein Inspired Coatings. *Adv. Mater.* 2009; 21:431. [PubMed: 19802352]
14. Sassolas A, Leca-Bouvier BD, Blum LJ. DNA Biosensors and Microarrays. *Chem. Rev.* 2007; 108:109. [PubMed: 18095717]
15. Stoughton, RB. *Annu. Rev. Biochem.* Vol. Vol. 74. Palo Alto: Annual Reviews; 2005. p. 53

16. Duggan DJ, Bittner M, Chen YD, Meltzer P, Trent JM. Expression Profiling Using Cdna Microarrays. *Nat. Genet.* 1999; 21:10. [PubMed: 9915494]
17. Debouck C, Goodfellow PN. DNA Microarrays in Drug Discovery and Development. *Nat. Genet.* 1999; 21:48. [PubMed: 9915501]
18. Brown PO, Botstein D. Exploring the New World of the Genome with DNA Microarrays. *Nat. Genet.* 1999; 21:33. [PubMed: 9915498]
19. Thiel AJ, Frutos AG, Jordan CE, Corn RM, Smith LM. In Situ Surface Plasmon Resonance Imaging Detection of DNA Hybridization to Oligonucleotide Arrays on Gold Surfaces. *Anal. Chem.* 1997; 69:4948.
20. Jordan CE, Frutos AG, Thiel AJ, Corn RM. Surface Plasmon Resonance Imaging Measurements of DNA Hybridization Adsorption and Streptavidin/DNA Multilayer Formation at Chemically Modified Gold Surfaces. *Anal. Chem.* 1997; 69:4939.
21. Brockman JM, Frutos AG, Corn RM. A Multistep Chemical Modification Procedure to Create DNA Arrays on Gold Surfaces for the Study of Protein-DNA Interactions with Surface Plasmon Resonance Imaging. *J. Am. Chem. Soc.* 1999; 121:8044.
22. He L, Musick MD, Nicewarner SR, Salinas FG, Benkovic SJ, Natan MJ, Keating CD. Colloidal Au-Enhanced Surface Plasmon Resonance for Ultrasensitive Detection of DNA Hybridization. *J. Am. Chem. Soc.* 2000; 122:9071.
23. Zhou W, Chen Y, Corn RM. Ultrasensitive Microarray Detection of Short Rna Sequences with Enzymatically Modified Nanoparticles and Surface Plasmon Resonance Imaging Measurements. *Anal. Chem.* 2011; 83:3897. [PubMed: 21524060]
24. Lee HJ, Wark AW, Corn RM. Enhanced Bioaffinity Sensing Using Surface Plasmons, Surface Enzyme Reactions, Nanoparticles and Diffraction Gratings. *Analyst.* 2008; 133:596. [PubMed: 18427679]
25. Lai YJ, Tseng WL. Role of 5-Thio-(2-Nitrobenzoic Acid)-Capped Gold Nanoparticles in the Sensing of Chromium(VI): Remover and Sensor. *Analyst.* 2011; 136:2712. [PubMed: 21589978]
26. Chen Y, Nguyen A, Niu L, Corn RM. Fabrication of DNA Microarrays with Poly(L-Glutamic Acid) Monolayers on Gold Substrates for Spr Imaging Measurements. *Langmuir.* 2009; 25:5054. [PubMed: 19253965]
27. Lee HJ, Li Y, Wark AW, Corn RM. Enzymatically Amplified Surface Plasmon Resonance Imaging Detection of DNA by Exonuclease Iii Digestion of DNA Microarrays. *Anal. Chem.* 2005; 77:5096. [PubMed: 16097744]
28. Hong S, Na YS, Choi S, Song IT, Kim WY, Lee H. Non-Covalent Self-Assembly and Covalent Polymerization Co-Contribute to Polydopamine Formation. *Adv. Funct. Mater.* 2012; 22:4711.
29. Peterson AW, Heaton RJ, Georgiadis RM. The Effect of Surface Probe Density on DNA Hybridization. *Nucleic Acids Res.* 2001; 29:5163. [PubMed: 11812850]
30. Sendroiu IE, Gifford LK, Lupták A, Corn RM. Ultrasensitive DNA Microarray Biosensing Via in Situ Rna Transcription-Based Amplification and Nanoparticle-Enhanced Spr Imaging. *J. Am. Chem. Soc.* 2011; 133:4271. [PubMed: 21391582]
31. Tawa K, Knoll W. Mismatching Base-Pair Dependence of the Kinetics of DNA-DNA Hybridization Studied by Surface Plasmon Fluorescence Spectroscopy. *Nucleic Acids Res.* 2004; 32:2372. [PubMed: 15115799]
32. Chen Y, Corn RM. Dnazyme Footprinting: Detecting Protein-Aptamer Complexation on Surfaces by Blocking Dnazyme Cleavage Activity. *J. Am. Chem. Soc.* 2013; 135:2072. [PubMed: 23351044]
33. Li Y, Liu M, Xiang C, Xie Q, Yao S. Electrochemical Quartz Crystal Microbalance Study on Growth and Property of the Polymer Deposit at Gold Electrodes During Oxidation of Dopamine in Aqueous Solutions. *Thin Solid Films.* 2006; 497:270.



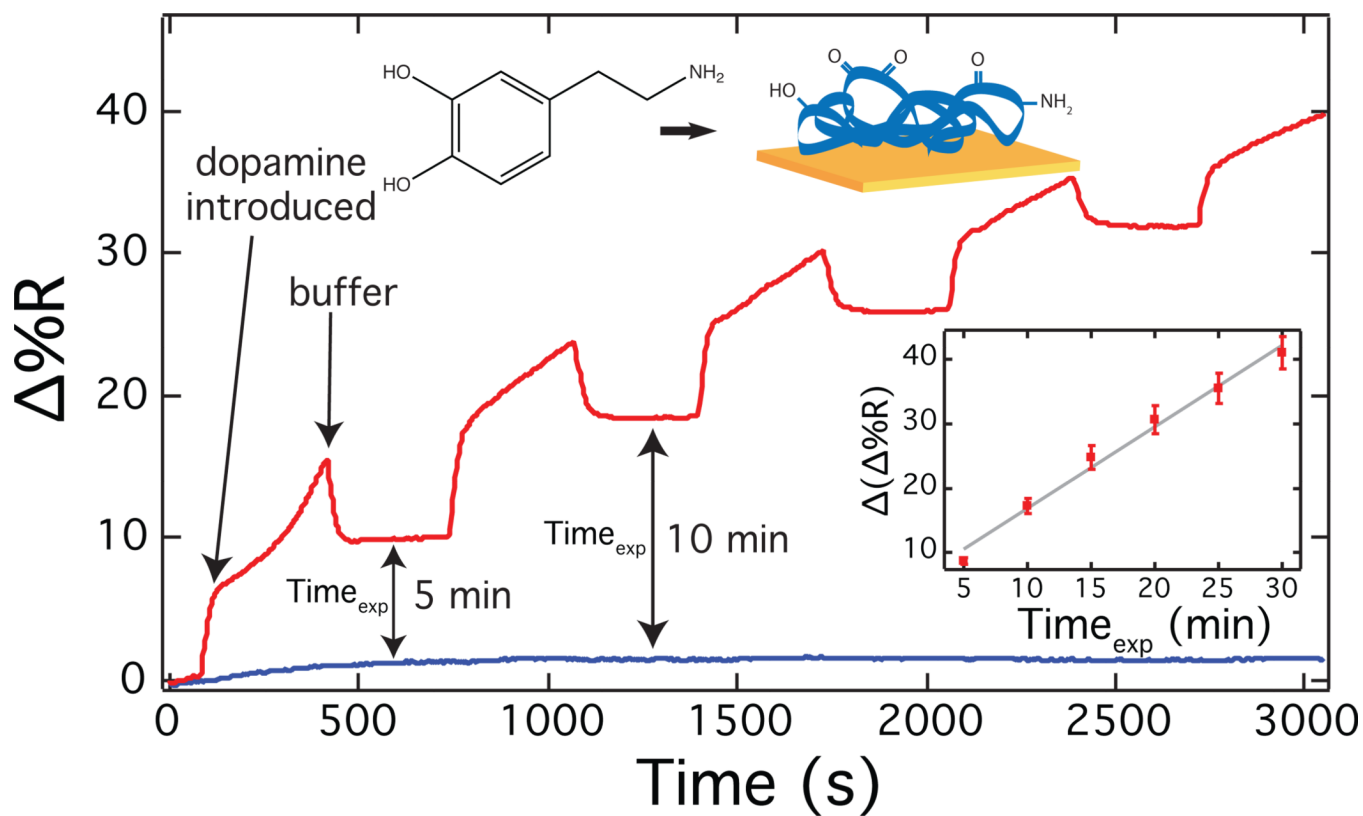


**Figure 1.** Real-time SPRI measurement of PDA film growth. Inset shows the linear relationship between growth time and reflectivity change.  $\text{Time}_{\text{exp}}$  denotes the cumulated time that the array surface has been exposed to dopamine solution.

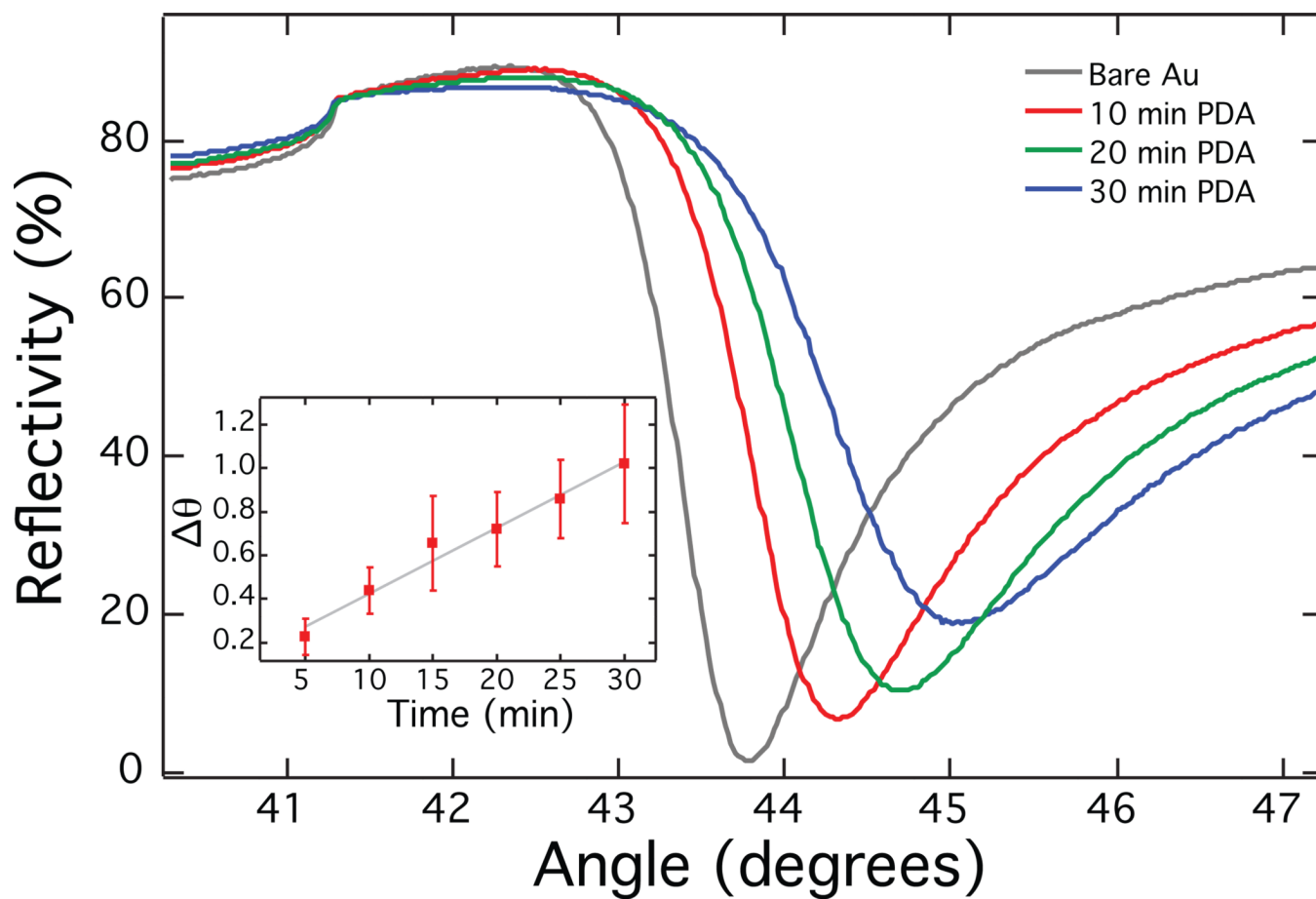


**Figure 2.** Scanning angle measurements show the shifts in angle minima as PDA deposition time lengthens. Inset displays the linear dependence of angle on film growth time.

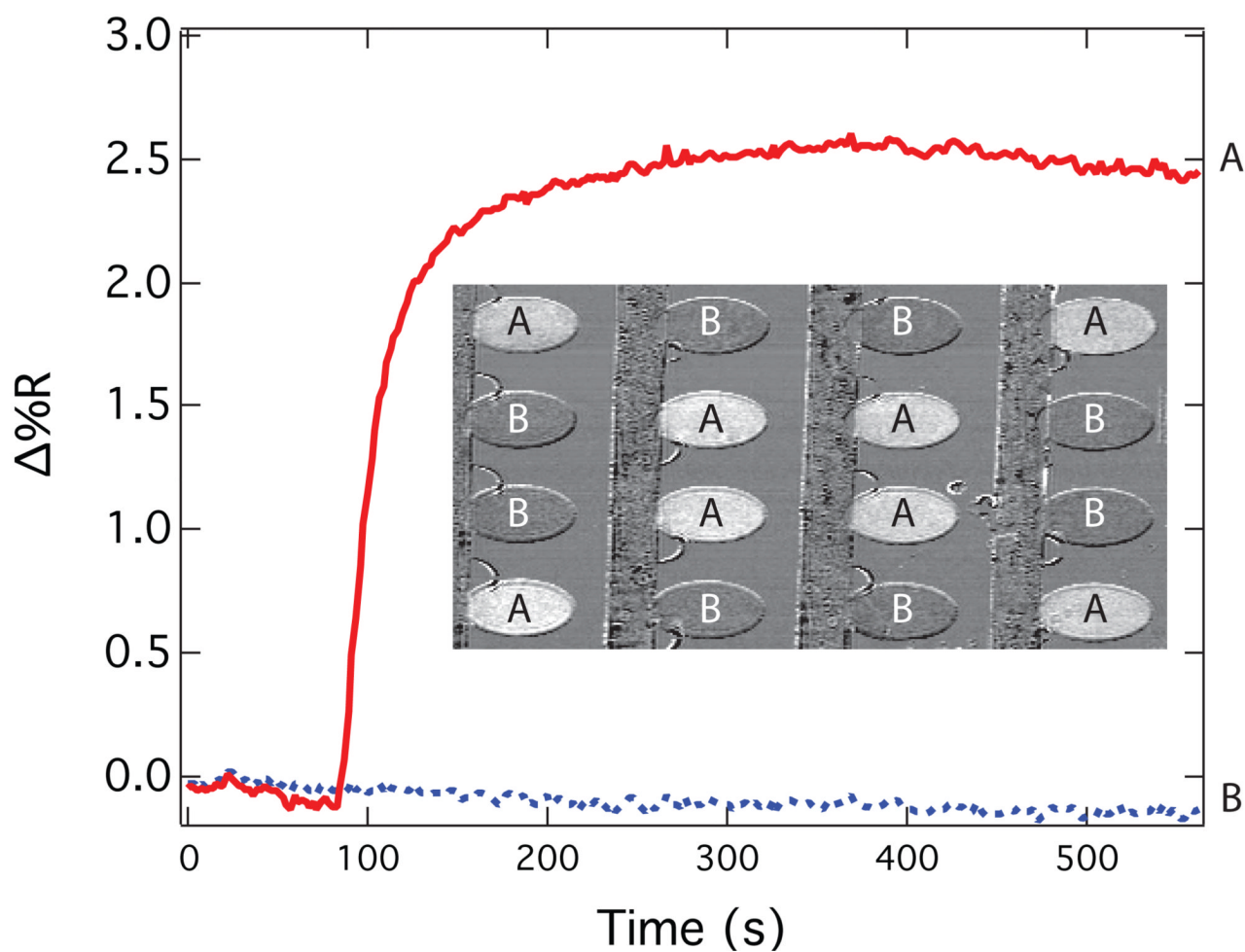


**Figure 3.** SPRI measurement of ssDNA hybridizing with its complementary counterpart (sequence A, solid curve) on the DNA microarray, giving 2.5 %R. The data also shows no nonspecific adsorption of ssDNA to the noncomplementary, control DNA (sequence B, dotted curve) on the microarray surface. The inset is the real-time SPRI difference image.

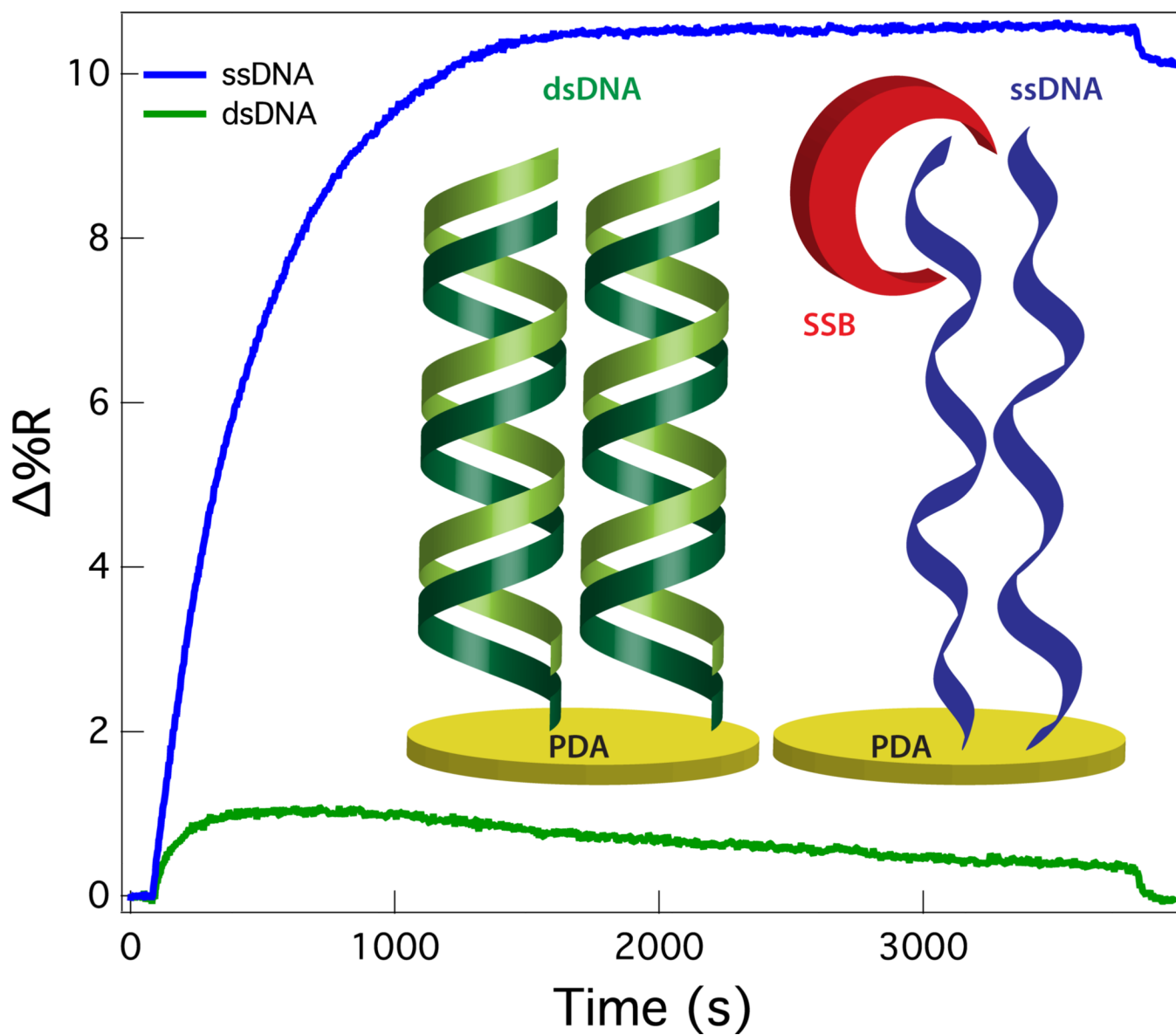


**Figure 4.** SPRI measurement of SSB binding onto ssDNA attached to PDA layer on the microarray.

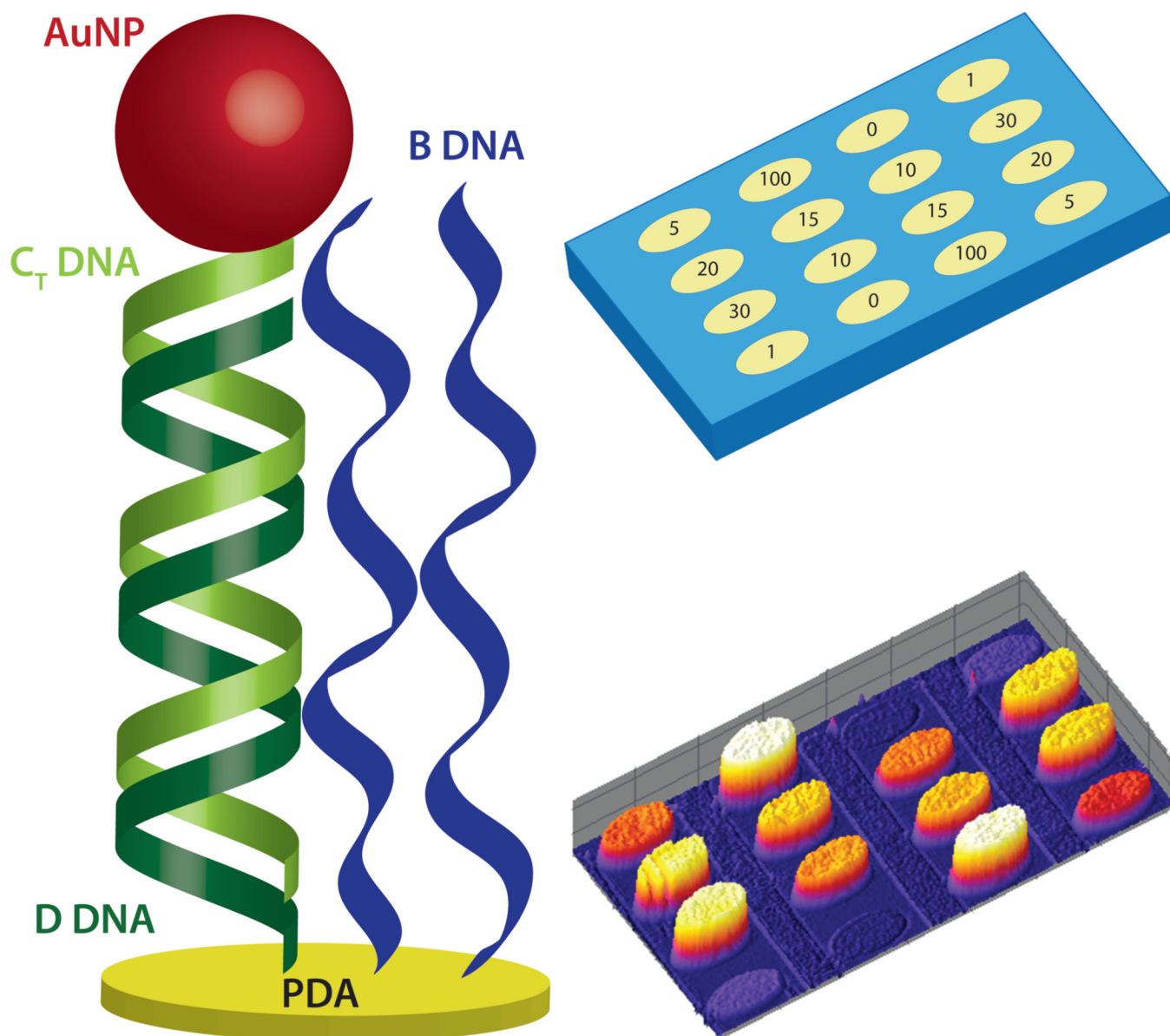


**Figure 5.** Schematic of  $C_T$  ssDNA-modified AuNPs hybridizing with D ssDNA. The mixed, two component spots were constructed by attaching ssDNA to the PDA layer. The numbers on the microarray represent the percentage of D ssDNA on the surface. Also shown is the real-time difference image of ssDNA microarray after signal saturation from  $C_T$ -AuNPs hybridization.

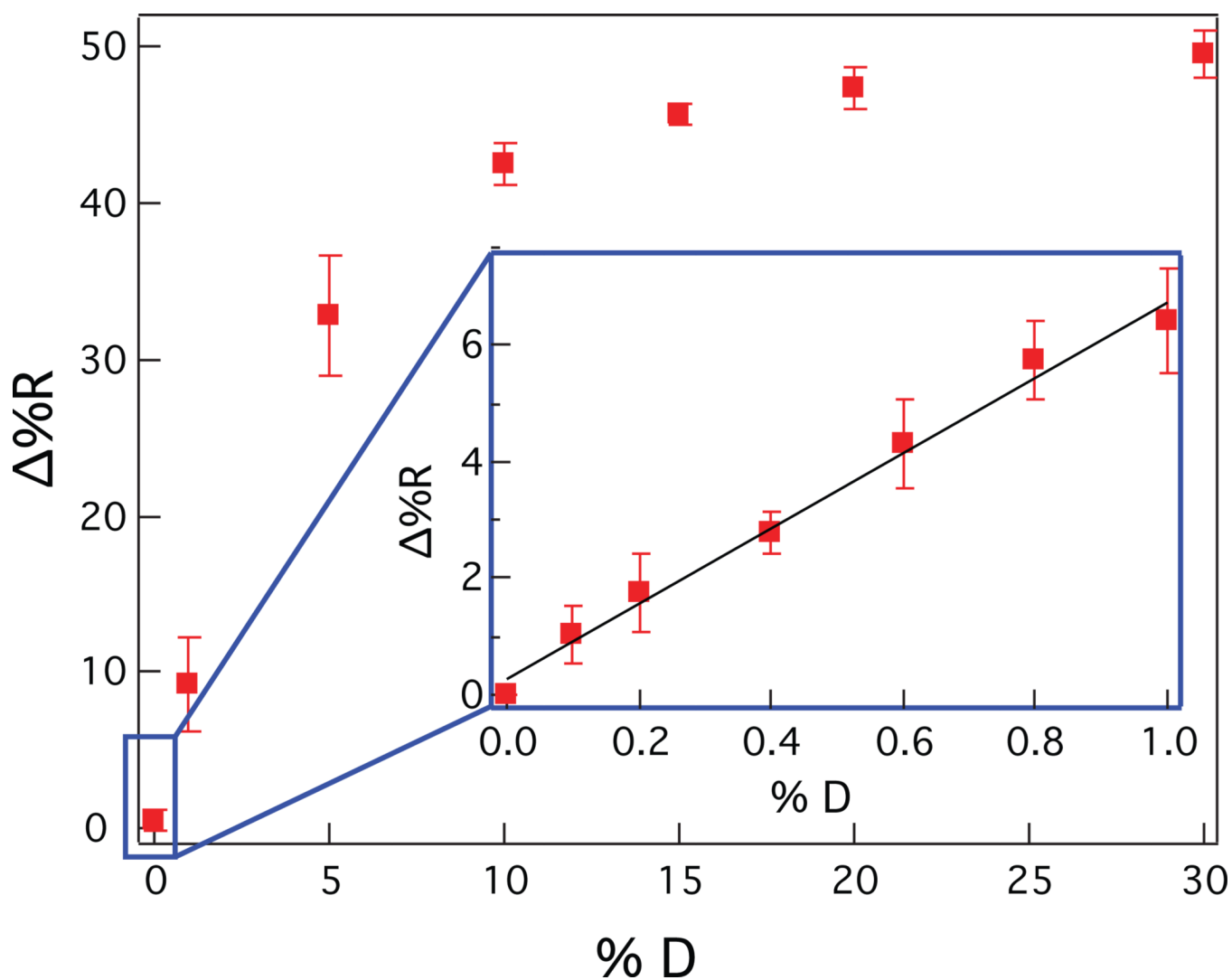


**Figure 6.** SPRi measurements of  $C_T$  ssDNA modified AuNPs hybridization onto ssDNA microarray built from PDA attachment chemistry. Inset shows the  $C_T$ -AuNPs hybridization onto the surfaces with 0% to 1% D ssDNA.

**Table 1**

DNA oligonucleotides employed in this paper

A	5'-NH <sub>2</sub> (CH <sub>2</sub> ) <sub>12</sub> CGAAATCCAGACACATAAGCACGAACCGAA-3'
B	5'-NH <sub>2</sub> (CH <sub>2</sub> ) <sub>12</sub> TTCGGTTCGTGCTTATGTGTCTGGATTTCG-3'
A <sub>C</sub>	5'-TTCGGTTCGTGCTTATGTGTCTGGATTTCG-3'
C	5'-NH <sub>2</sub> (CH <sub>2</sub> ) <sub>12</sub> A <sub>30</sub> -3'
C <sub>T</sub>	5'-S-S(CH <sub>2</sub> ) <sub>6</sub> A <sub>30</sub> -3'
D	5'-NH <sub>2</sub> (CH <sub>2</sub> ) <sub>12</sub> T <sub>30</sub> -3'
D <sub>U</sub>	5'-T <sub>30</sub> -3'